Electronic Journal of Differential Equations, Vol. 2017 (2017), No. 01, pp. 1–21.
ISSN: 1072-6691. URL: http://ejde.math.txstate.edu or http://ejde.math.unt.edu

OPTIMAL MANAGEMENT AND SPATIAL PATTERNS IN A DISTRIBUTED SHALLOW LAKE MODEL

DIETER GRASS, HANNES UECKER

Abstract. We present a numerical framework to treat infinite time horizon spatially distributed optimal control problems via the associated canonical system derived by Pontryagin's maximum principle. The basic idea is to consider the canonical system in two steps. First we perform a bifurcation analysis of canonical steady states using the continuation and bifurcation package `pde2path`, yielding a number of so called flat and patterned canonical steady states. In a second step we link `pde2path` to the two point boundary value problem solver `TOM` to study time dependent canonical paths to steady states having the so called saddle point property. As an example we consider a shallow lake model with diffusion.

1. Introduction

Many intertemporal optimization problems in applied science, specifically economics, are described by optimal control (OC) problems with an infinite time horizon where the state dynamics are given by some ordinary differential equation (ODE) [10, 12, 19]. One central method of solution of such OC problems is Pontryagin's maximum principle [30], where the so called canonical system, consisting of the state ODE and an associated adjoint ODE for the co–states, is derived as a necessary optimality condition, and where for the infinite horizon case a crucial point are the so called limiting transversality conditions for $t \to \infty$ [4, 5, 36].

For optimal control problems with the states fulfilling a partial differential equation (PDE), the theory is well developed in the stationary case, or for evolutionary problems over finite time horizons $[0, T]$, where some conditions at the final time T need to be imposed. See, e.g., [31, 32, 37], or [1, Chapter 5], and §2.2 for further references. However, a strict mathematical proof of Pontryagin's maximum principle in the PDE setting over an infinite time horizon is still missing. Nevertheless, in [9] this approach has been transfered to OC problems involving diffusion, and after the formal derivation of the canonical systems for some example problems the authors show the remarkable result that under certain conditions on the Hamiltonian there occurs a Turing like bifurcation from flat to patterned steady states of the canonical system, and call this phenomenon optimal diffusion-induced instability.

Here we present a numerical framework to (a) study such bifurcations of canonical steady states numerically in a simple way, and (b) study their optimality by

2010 *Mathematics Subject Classification.* 49J20, 49N90, 35B32.
Key words and phrases. Optimal control; Pontryagin's maximum principle; bioeconomics; canonical steady states; connecting orbits.

Submitted June 10, 2015. Published January 4, 2017.

computing and evaluating time-dependent canonical paths to such canonical steady states. As a model problem we consider one of the three examples presented in [9], namely a version of the, in the field of ecological economics, well-known shallow lake optimal control (SLOC) model, cf. [33, 26, 11].

We use the acronyms FCSS and PCSS for flat and patterned canonical steady states, respectively. The SLOC model has up to three (branches of) FCSS in relevant parameter regimes, and in these regimes we also find a large number of (branches of) PCSS. In this situation of multiple canonical steady states a local stability analysis at a given canonical steady state is in general not sufficient to discuss their optimality. Here, local stability analysis means that the stationary canonical system is analyzed, analogous to a steady-state analysis of the canonical system in the ODE setting. It is well known and shown for many models that the appearance of multiple canonical steady states (even if these steady-states are saddle-points) does not necessarily imply the appearance of multiple steady-states in the optimal system, cf. [19, 21]. The reason is that there can exist non–constant extremal solutions, i.e. canonical paths connecting the state values of a given canonical steady state to some other canonical steady state, and yielding a higher objective value. Therefore, to study whether a canonical steady state is optimal, the values of canonical paths also have to be considered.

Here we numerically compute the bifurcation behavior of FCSS and PCSS for the diffusive SLOC model in some detail, and study their optimality by evaluation of their objective values J and comparison to time-dependent canonical paths. Such a global analysis is inevitable and has to accompany the local stability analysis. Since in general the pertinent ODEs or PDEs cannot be solved analytically we have to use numerical methods for the calculation of FCSS and in particular PCSS, and for the calculation of canonical paths. For the steady state problem we use the continuation and bifurcation software `pde2path` [41], based on a spatial finite element method discretization, which we then combine with the boundary value problem (BVP) solver TOM to obtain canonical paths.

A standard reference on ecological economics or "Bioeconomics" is [12], which also contains a very readable account, and applications, of Pontryagin's maximum principle in the context of ODE models, while [19] focuses more on socio–economical ODE model applications. Besides in [9], and in [7], PDE models roughly similar to our diffusive SLOC model are considered in, e.g., [22, 1, 13, 2, 3], partly including numerical simulations. However, these works are in a finite time horizon setting, and with control constraints, which altogether gives a rather different setting from the one considered here. See Remark 2.2 for further comments.

In §2 we present the SLOC model. To give some background, in §2.1 we briefly present the 0D (ODE) version, and some basic concepts of optimal control, in particular Pontryagin's maximum principle. In §2.2 we turn to the distributed case and explain the associated canonical system. In §3 we explain the numerics to first compute the bifurcation diagram of canonical steady states, and then find canonical paths. We mostly focus on one spatial dimension (1D), but also give a short outlook on the 2D case. It turns out that in the parameter regimes studied here the PCSS are not optimal, but nevertheless they play a relevant role. Moreover, calculating *optimal* canonical paths to FCSS yields interesting and to some extent counter–intuitive information about the optimal control of the distributed SLOC model.

In §4 we close with a short summary and discussion, and the Appendix contains remarks about the saddle point property for canonical steady state in a PDE setting, starting on the discretized level.

Our software, including demo files and a manual to run some of the simulations in this paper, can be downloaded at [40]. In fact, the present paper is the first in a series of four related works, the other three being [38, 18, 39]: [38] contains a Quickstart guide and implementation details of the add on package `p2poc` to `pde2path` used for the computations in this paper. Thus, the reader interested in these details should read (parts of) [38] in parallel. Next, [18] explains the usage of `OCMat` to study 1D distributed OC problems based on spatial finite difference approximations, with the same SLOC model as in the present paper as an example, and thus obtaining comparable results, but also studying a second parameter regime. Finally, in [39] we apply `p2poc` to an OC problem for a reaction–diffusion system modeling a vegetation-water-harvesting interaction. In contrast to the SLOC model studied here, this yields dominant patterned optimal steady states in wide parameter regimes, and thus interesting new results on spatial patterns in optimal harvesting.

2. Model and background from optimal control

2.1. **Shallow lake model without diffusion.** A well known non–distributed or 0D version of the SLOC model, see e.g. [42], can be formulated in dimensionless form as

$$V(P_0) := \max_{k(\cdot)\geq 0} J(P_0, k(\cdot)), \tag{2.1a}$$

$$J(P_0, k(\cdot)) := \int_0^\infty \mathrm{e}^{-rt} J_c(P(t), k(t))\,\mathrm{d}t, \tag{2.1b}$$

where

$$J_c(P, k) = \ln k - \gamma P^2 \tag{2.1c}$$

is the current value objective function, and P satisfies the ODE initial value problem

$$\dot{P}(t) = k(t) - bP(t) + \frac{P(t)^2}{1 + P(t)^2}, \quad P(0) = P_0 \geq 0. \tag{2.1d}$$

Here $r, \gamma, b > 0$ are parameters, $P = P(t)$ is the phosphorus contamination of the lake, which we want to keep low for ecological reasons, and $k = k(t)$ is the phosphate load, for instance from fertilizers used by farmers, which farmers want high for economic reasons. The objective function consists of the concave increasing function $\ln k$, and the concave decreasing function $-\gamma P^2$; b is the phosphorus degradation rate in the lake, and r is the discount rate. The discounted time integral in (2.1b) is typical for economic (or socio-political) problems, where "profits now" weight more than mid or far future profits. More specifically, r often corresponds to a long-term investment rate. Following [42] we focus on the parameter choice

$$r = 0.03, \quad \gamma = 0.5, \quad b \in (0.5, 0.8) \quad \text{(primary bifurcation parameter)}, \tag{2.2}$$

which is mainly motivated by the fact that in this regime the model has so called Skiba points, see §3.3.2. The max in (2.1b) runs over all *admissible* controls k and (associated) states P; for k we can take the space $C_b^0([0,\infty),[0,\infty))$, and for P the space $C_b^1([0,\infty),\mathbb{R})$. In fact, we naturally have $k(t) > 0$ for all t as $J_c(k, P) \to -\infty$

as $k \searrow 0$ and the equilibrium $\hat{P} = \hat{k} = 0$ is not optimal, cf. [42]. Thus, one can choose some $\varepsilon > 0$ and restrict the admissible controls to satisfy $k(t) \geq \varepsilon$.

By Pontryagin's maximum principle [30], see also [19], an optimal solution $(P^*(\cdot), k^*(\cdot))$ has to satisfy the first order optimality conditions

$$k^*(t) = \operatorname{argmax}_k \mathcal{H}(P(t), k, q(t), q_0) \quad \text{for almost all } t \geq 0, \tag{2.3a}$$

with the local current value Hamiltonian function

$$\mathcal{H}(P, k, q, q_0) := q_0 J_c(P, k) + q\left(k - bP + \frac{P^2}{1+P^2}\right). \tag{2.3b}$$

The state $P(\cdot)$ and costate $q(\cdot)$ paths are solutions of the canonical system

$$\dot{P}(t) = \partial_q \mathcal{H}(P(t), k^*(t), q(t)) = k^*(t) - bP(t) + \frac{P(t)^2}{1+P(t)^2}, \tag{2.4a}$$

$$\begin{aligned} \dot{q}(t) &= rq(t) - \partial_P \mathcal{H}(P(t), k^*(t), q(t)) \\ &= 2\gamma P(t) + q(t)\Big(r + b - \frac{2P(t)}{(1+P(t)^2)^2}\Big), \end{aligned} \tag{2.4b}$$

with $P(0) = P_0 > 0$, additionally satisfying the transversality condition

$$\lim_{t\to\infty} \mathrm{e}^{-rt} P(t) q(t) = 0. \tag{2.5}$$

It can be proved that the problem is normal, i.e. $q_0 > 0$, and hence w.l.o.g. $q_0 = 1$ can be assumed and is therefore subsequently omitted.

A solution $(P(\cdot), q(\cdot))$ of the canonical system (2.4) is called a *canonical path*, and a steady state of (2.4) is called a *canonical steady state*. Because of the strict concavity and continuous differentiability of the Hamiltonian function with respect to the control k, and the absence of control constraints, the solution of (2.3a) is given by

$$\partial_k \mathcal{H}(P(t), k(t), q(t)) = 0, \tag{2.6}$$

which yields $k^*(t) = -1/q(t)$.

Consequently, for $(P(\cdot), q(\cdot))$ a canonical path, i.e., a solution of the canonical system, with a slight abuse of notation we also call (P, k) with $k = -1/q$ a canonical path. In particular, if $(\hat{P}, \hat{q})$ is a canonical steady state, so is $(\hat{P}, \hat{k})$. Canonical paths yield candidates for optimal solutions, defined as follows:

Definition 2.1. $(P^*(\cdot), k^*(\cdot, P_0))$ is called an optimal solution of (2.1a) if for every admissible $k(\cdot)$ and associated $P(\cdot)$ we have

$$J(P_0, k(\cdot)) \leq J(P_0, k^*(\cdot, P_0)) = V(P_0).$$

Then $k^*(\cdot, P_0)$ is called an *optimal control*, $P^*(\cdot)$ is called the corresponding *optimal (state) path*, and

$$\dot{P}(t) = k^*(t, P_0) - bP(t) + \frac{P(t)^2}{1+P(t)^2} \tag{2.7}$$

is called the *optimal ODE*. A constant solution $(P^*(\cdot), k^*(\cdot, P_0)) \equiv (\hat{P}, \hat{k}(\hat{P}))$ of (2.7) is called an *optimal steady state*.

It turns out that the long-run behavior of an optimal solution $(P^*(\cdot), k^*(\cdot))$ can be characterized completely, see, e.g., [42]. Each optimal solution converges to an optimal steady state, and depending on the parameters (2.4) can have $I = 1, 2, 3$ canonical steady state $(\hat{P}, \hat{q})_i$, $i = 1, \ldots, I$. cf., e.g., the FCSS branches in Figure 1 for our specific parameter choice.

For simplicity omitting the non-generic case $I = 2$, if $I = 1$ then the unique canonical steady state is a globally stable optimal steady state, while for $I = 3$ two canonical steady state are locally stable optimal steady states, and the third is unstable. Here, an optimal steady state $(\hat{P}, \hat{q})$ is called globally (locally) stable if for each $P(0)$ (in a neighborhood of $\hat{P}$) the associated optimal path converges to $(\hat{P}, \hat{q})$; see [21, 20] for a detailed discussion.

Setting

$$u := (P, q),$$

and letting $\hat{u}$ be a steady state of (2.4), the problem now is to compute a path, or "connecting orbit", with $P(0) = P_0$ and $\lim_{t\to\infty} u(t) = \hat{u}$. One standard approach, see, e.g. [23, 15, 6] and in particular [19, Chapter 7], is to treat (2.4) on a finite time interval $[0, T]$ and to require $u(T) \in W_s(\hat{u})$, where $W_s(\hat{u})$ is the local stable manifold of $\hat{u}$. In practice we approximate $W_s(\hat{u})$ by the stable eigenspace $E_s(\hat{u})$, and thus require

$$u(T) \in E_s(\hat{u}) \quad \text{and close to } \hat{u}. \tag{2.8}$$

To obtain a well defined two point boundary value problem we need $\dim E_s(\hat{u}) = 1$. We now generalize this to distributed problems, and thus in §3 explain further details on that level.

2.2. **Shallow lake model with diffusion.** Following [9] we consider the shallow lake model with diffusion in a domain $\Omega \subset \mathbb{R}^d$, $d = 1, 2$, i.e.,

$$\begin{aligned} V(P_0(\cdot)) &:= \max_{k(\cdot,\cdot)\geq 0} J(P_0(\cdot), k(\cdot,\cdot)), \\ J(P_0(\cdot), k(\cdot,\cdot)) &:= \int_0^\infty \mathrm{e}^{-rt} J_{ca}(P(t), k(t))\,\mathrm{t}, \end{aligned} \tag{2.9a}$$

where

$$J_{ca}(P(\cdot,t), k(\cdot,t)) = \frac{1}{|\Omega|}\int_\Omega J_c(P(x,t), k(x,t))\,\mathrm{d}x \tag{2.9b}$$

is the spatially averaged current value objective function (with $J_c(P,k) = \ln k - \gamma P^2$ as before), and P fulfills the initial boundary value problem

$$\partial_t P(x,t) = k(x,t) - bP(x,t) + \frac{P(x,t)^2}{1+P(x,t)^2} + D\Delta P(x,t), \tag{2.9c}$$

$$\partial_\nu P(x,t)\big|_{\partial\Omega} = 0, \quad P(x,t)\big|_{t=0} = P_0(x), \quad x \in \Omega \subset \mathbb{R}^d, \tag{2.9d}$$

where $\Delta = \partial^2_{x_1} + \ldots + \partial^2_{x_d}$, and ν is the outer normal of Ω.

We normalize J_{ca} by the domain size $|\Omega|$ for easy comparison between the 0D, 1D, and 2D cases, and, more generally, between different domains. We mostly focus on $\Omega = (-L, L)$ a real interval, but also give an outlook to 2D. In 2D the model is somewhat less intuitive, as a controlled phosphate dumping in the "middle" of the lake from farming appears difficult to motivate, and thus in 2D we rather think of (2.9) as a general pollution model. Instead of the periodic boundary conditions (BC) in 1D in [9] we require Neumann (zero flux) BC, which from a modeling point of view we find more reasonable because a body of water with torus geometry is somewhat unnatural, in particular in 2D.

Introducing the costate $q : \Omega \times (0,\infty) \to \mathbb{R}^N$ and the (local current value) Hamiltonian

$$\mathcal{H} = \mathcal{H}(P, q, k) = J_c(v, k) + q\big[k - bP + \frac{P^2}{1+P^2} + D\Delta P\big], \tag{2.10}$$

by techniques of optimal control for PDE from [25, 24], typically again called Pontryagin's maximum principle, one may formally (see Remark 2.2) derive a canonical system for (2.9), which reads

$$\partial_t P(x,t) = [\partial_q \mathcal{H}](x,t) = k(x,t) - bP(x,t) + \frac{P(x,t)^2}{1+P(x,t)^2} + D\Delta P(x,t), \tag{2.11a}$$

$$\begin{aligned}\partial_t q(x,t) &= rq(x,t) - [\partial_P \mathcal{H}](x,t)\\ &= 2\gamma P(x,t) + q(x,t)\Big(r + b - \frac{2P(x,t)}{(1+P(x,t)^2)^2}\Big) - D\Delta q(x,t),\end{aligned} \tag{2.11b}$$

$$\partial_\nu P(x,t)\big|_{\partial\Omega} = 0, \quad \partial_\nu q(x,t)\big|_{\partial\Omega} = 0, \quad P(x,t)\big|_{t=0} = P_0(x), \quad x \in \Omega, \tag{2.11c}$$

where $k = \operatorname{argmax}_{\tilde{k}} \mathcal{H}(P,q,\tilde{k})$, which similar to (2.6) is obtained from

$$\partial_k \mathcal{H}(P,q,k) = 0 \quad \Leftrightarrow \quad k(x,t) = -\frac{1}{q(x,t)}. \tag{2.11d}$$

The costate q also fulfills zero flux BC, and derivatives like $\partial_P \mathcal{H}$ etc are taken variationally, i.e., for

$$\overline{\mathcal{H}}(t) = \int_\Omega \mathcal{H}(P(x,t), p(x,t), k(x,t))\,\mathrm{d}x. \tag{2.12}$$

For instance, for $\Phi(P,q) := q\Delta P$ we have $\overline{\Phi}(P,q) = \int_\Omega q\Delta P\,\mathrm{d}x = \int_\Omega (\Delta q)P\,\mathrm{d}x$ by Gauß' theorem, hence $\delta_P\overline{\Phi}(P,q)[h] = \int(\Delta q)h\,\mathrm{d}x$, and by the Riesz representation theorem we identify $\delta_P\overline{\Phi}(P,q)$ and hence $\partial_P\Phi(P,q)$ with the multiplier Δq.

Finally, we impose the transversality condition

$$\lim_{t\to\infty} \mathrm{e}^{-rt}\int_\Omega q(x,t)P(x,t)\,\mathrm{d}x = 0, \tag{2.13}$$

which is needed for going from the Lagrangian (see [8, Appendix])

$$\begin{aligned}\mathcal{L}(P,q,k) = \int_0^\infty \mathrm{e}^{-rt}\Big[\int_\Omega J_c(P,k)\\ - q\Big(\partial_t P - \big(k - bP + \frac{P^2}{1+P^2} + D\Delta P\big)\Big)\,\mathrm{d}x\Big]\,\mathrm{d}t\end{aligned}$$

to the Hamiltonian $\tilde{\mathcal{H}} = \int_0^\infty \mathrm{e}^{-rt}\overline{\mathcal{H}}(t)\,\mathrm{d}t$, i.e., for integration by parts in t to obtain

$$\begin{aligned}&-\int_0^\infty \mathrm{e}^{-rt}\int_\Omega q(x,t)\partial_t P(x,t)\,\mathrm{d}x\,\mathrm{d}t\\ &= \int_\Omega q(x,0)P(x,0)\,\mathrm{d}x + \int_0^\infty \mathrm{e}^{-rt}\int_\Omega P(x,t)(\partial_t q(x,t) - rq(x,t))\,\mathrm{d}x\,\mathrm{d}t.\end{aligned}$$

We now give a definition analogous to Definition 2.1, which however is somewhat ad hoc, because for instance we refrain from giving function spaces for (P,q), or (P,k), and hence use "admissible" in a heuristic sense $k(x,t) > 0$ for all $x \in \Omega, t \in [0,\infty)$. In fact, ultimately we will only consider (2.11) as a system of ODEs after spatial discretization, see also Remark 2.2.

Heuristic definition Let $(P^*(\cdot,\cdot), k^*(\cdot,\cdot,P_0))$ be an optimal solution of problem (2.9), i.e. for every admissible $k(\cdot,\cdot)$ and associated $P(\cdot,\cdot)$ we have

$$J(P_0, k(\cdot,\cdot)) \le J(P_0, k^*(\cdot,\cdot,P_0)) = V(P_0).$$

Then $k^*(\cdot,\cdot,P_0)$ is called a (distributed) *optimal control*, $P^*(\cdot,\cdot)$ is called the associated distributed *optimal (state) path*, and

$$\begin{aligned} \partial_t P(x,t) &= k^*(x,t,P_0(x)) - bP(x,t) + \frac{P(x,t)^2}{1+P(x,t)^2} + D\Delta P(x,t), \\ \partial_\nu P(x,t)\big|_{\partial\Omega} &= 0, \end{aligned} \tag{2.14}$$

is called the *optimal PDE*. Again with a slight abuse of notation, (P^*,k^*) is also called an optimal path, and an optimal stationary solution $(\hat{P}(\cdot),\hat{k}(\cdot))$ of (2.11) is called an *optimal steady state*. If $\hat{P}(\cdot)\equiv\hat{P}$ then the optimal steady state is called a *flat optimal steady state*, otherwise it is called a *patterned optimal steady state*.

For convenience we let $u=(P,q)$, and call solutions $u(\cdot,\cdot)$ of (2.11) canonical paths, and steady states $\hat{u}(\cdot)$ of (2.11) canonical steady states. Moreover, we use the acronyms FCSS for flat canonical steady states ($\hat{u}(\cdot)\equiv\hat{u}$) and PCSS (patterned canonical steady state) otherwise. Obviously, the FCSS correspond precisely to the 0D canonical steady state from §2.1. It was already indicated in [9] that (2.11) can additionally have PCSS arising from Turing like bifurcations. Thus, we first calculate bifurcation diagrams of steady states for (2.11), in 1D and 2D, recovering the up to 3 branches of FCSS from §2.1, and many branches of PCSS. Next, analogous to the 0D case, we expect a solution of (2.9) to converge to some canonical steady state $\hat{u}$. Thus, we only consider solutions $u(\cdot,\cdot)$ of (2.11) with $\lim_{t\to\infty}u(\cdot,t)=\hat{u}(\cdot)$, where $\hat{u}(\cdot)$ is a canonical steady state.

Remark 2.2. (a) As already said in the Introduction, a strict mathematical proof of Pontryagin's maximum principle for diffusion problems over infinite time horizons is still missing, specifically for the transversality condition (2.13), which in the Appendix of [8] was used to derive (2.11) from $\mathcal{L}$ by the above formal variational argument. Alternatively, one could first discretize (2.9) in space and then for a given discretization for instance apply the theory from [36] to obtain a spatially discrete version of (2.11), and the transversality condition in [36, Corollary 4.1]. In the spatially discrete sense this is equivalent to (2.13). The crucial assumption ($\mathbf{A_2}$) from [36] holds for k bounded away from zero, and as in the 0D case in §2.1 we expect this to hold due to term $\ln k$ in the objective function, which in particular yields that no optimal steady state with $k(x)=0$ for some $x\in\Omega$ exists. Of course, to obtain a rigorous argument from [36] for the *PDE* problem (2.9), the constants in [36] must be controlled uniformly in the discretization, and we refrain from this analysis here. Thus, at the moment apply Pontryagin's maximum principle in an ad hoc sense.

(b) See also [31, 32, 13, 2] and in particular [24, Chapter 4] and [1, Chapter 5] for Pontryagin's maximum principle for OC problems for semilinear parabolic state evolutions. However, these works are in a finite time horizon setting, and often the objective function is linear in the control and there are control constraints, e.g., $k(x,t)\in K$ with some bounded interval K. Therefore k is not obtained from the analogue of (2.11d), but rather takes values from ∂K, which is usually called bang–bang control. In, e.g., [29] and [14], stationary spatial OC problems for a fishery model with (active) control constraints are considered, including numerical simulations, which correspond to our calculation of canonical steady states for the SLOC model. Here we do not (yet) consider explicit control or state constraints, and have an objective function strictly concave in the control, and thus we have a rather different setting than the above works.

(c) We summarize that we do not aim at new theoretical PDE results, but rather consider (2.11) after a spatial discretization as a (large) ODE problem. Moreover, we specifically assume, based on the results for the 0D shallow lake model, that canonical paths converge to canonical steady state s, and therefore make no use of the "critical" transversality condition (2.13).[1] Thus, we first compute a detailed bifurcation diagram of canonical steady states, and then aim to find orbits connecting general initial states to these steady states. This means that we take a broader perspective than computing just one (possibly non–unique) optimal control, given an initial condition P_0. Instead, our method aims to give a somewhat global picture by identifying the pertinent canonical steady states and their respective domains of attraction.

3. Numerical algorithm and results

The general idea is to use a method of lines discretization of (2.11), i.e., to approximate

$$u(x,t) := (P(x,t), q(x,t)) = \sum_{i=1}^{2n} u_i(t)\phi_i(x), \tag{3.1}$$

where $(\phi_i)_{i=1,\dots,2n}$ spans a subspace X_n of the phase space X of (2.11), e.g., here $X = [H^1(\Omega)]^2$, and (u_i, u_{n+i}), $i = 1,\dots,n$, are the expansion coefficients of P, q, respectively. This converts (2.11) into a (high dimensional) ODE

$$\dot{u}(t) = -G(u(t)), \quad u_i(0) = u_{0,i}, \quad i = 1,\dots,n, \tag{3.2a}$$

for the coefficient vector $u = (u_i)_{i=1,\dots,2n}$, where we have initial data for exactly half of the expansion coefficients. We choose a truncation time T and augment (3.2a) with the approximate transversality condition

$$u(T) \in E_s(\hat{u}), \quad \text{and } \|u(T) - \hat{u}\| \text{ small}, \tag{3.2b}$$

where $\hat{u}$ is a steady state of (3.2a), and $E_s(\hat{u})$ is spanned by the eigenvectors of $-\partial_u G$ belonging to eigenvalues with negative real parts. To choose an arbitrary initial point in the state space we then need

$$\dim E_s(\hat{u}) = \dim E_u(\hat{u}), \tag{3.3}$$

which gives rise to the following definition.

Definition 3.1. A canonical steady state $\hat{u} \in \mathbb{R}^{2n}$ with $n_s := \dim E_s(\hat{u}) = n$ is called a *saddle point* canonical steady state. The number $\mathrm{d}(\hat{u}) := n - n_s$ is called the *defect* of $\hat{u}$, and a canonical steady state $\hat{u}$ with defect $d(\hat{u}) > 0$ is called *defective*.

In Section 5 we show that always $d(\hat{u}) \geq 0$, explain that $d(\hat{u})$ is mesh-independent for well resolved meshes, and discuss possible extension of the saddle point property $d(\hat{u}) = 0$ to PDEs, which is not straightforward since $E_s(\hat{u})$ (and $W_s(\hat{u})$) and $E_u(\hat{u})$ (and $W_u(\hat{u})$) are infinite dimensional for the PDE case. Here we first continue with the discretized system (3.2a). Arguably, the simplest discretization for (3.1), at least in 1D, is a finite difference scheme, which has the advantage that we can

[1] As noted in §2.1, for the 0D SLOC problem (2.1a) all canonical paths converge to a steady state; in particular, (2.4) has no periodic orbits, and this can be proven analytically via Poincaré–Bendixon, see [42]. For the distributed model (2.11), or its high-dimensional ODE counterpart via spatial discretization, we cannot rule out periodic orbits a priori, but we found no Hopf bifurcations in the (numerical) bifurcation analysis in §3.

directly use `OCMat` for (3.2a), (3.2b), see [18]. However, here we opt for a finite element ansatz for (3.1), using the setting of `pde2path` [41, 16] for two reasons:

(1) We want to consider (2.9) and hence (2.11) also on general 2D domains, and for more general models where the state variables may be vector valued functions already, see §4, again in 1D or 2D. In all these cases, finite differences and the coding of the respective spatially discrete systems may become rather cumbersome, while `pde2path` provides convenient interfaces precisely for such systems. Moreover, for more complicated systems adaptive meshes may become important, which are more easily handled in a finite element discretization, and are already an integral part of `pde2path`. (2) As explained above, the canonical system may have many stationary states; it is thus desirable to use a continuation and bifurcation package to find canonical steady state s. The goal then is to "seamlessly" link the setting of `pde2path` for stationary problems with boundary value problem (BVP) solvers for (3.2).

On the other hand, a drawback of spatial finite element discretizations is that the associated evolutionary problems have the natural form

$$M\dot{u}(t) = -Ku(t) + MF(u(t)) =: -G(u(t)), \tag{3.4}$$

where u corresponds to the nodal values, $M, K \in \mathbb{R}^{2n\times 2n}$ are called the mass matrix and the stiffness matrix, respectively, and $F : \mathbb{R}^{2n} \to \mathbb{R}^{2n}$ is the nonlinearity. The "-" signs in (3.4) comes from the convention that `pde2path` discretizes $-\Delta$ as K (positive definite).

The occurrence of M on the left hand side of (3.4) creates problems for the usage of standard BVP solvers. Thus we modified routines from the BVP solver TOM [28, 27] to handle M on the left hand side. For speedup it is advisable to avoid numerical differentiation and hence to pass a Jacobian function $\partial_u G =$ `fjac(t,u)` to TOM, additionally to the right side G from (3.4). This is generically very easy as `pde2path` already provides a fast and easy way to assemble Jacobians. See [38] for implementation details.

3.1. **Computing paths to saddle point canonical steady state s.** To calculate canonical paths from a given state P_0 that connect to some saddle point canonical steady state $\hat{u}$ we want to solve the two-point BVP

$$M\dot{u}(t) = -G(u(t)), \quad t \in (0,T), \tag{3.5a}$$

$$P_i(0) = P_{0,i}, \quad i = 1,\dots,n, \quad (n \text{ left BC}), \tag{3.5b}$$

$$\Psi(u(T) - \hat{u}) = 0 \in \mathbb{R}^n \quad (n \text{ right BC}), \tag{3.5c}$$

where $\Psi \in R^{n\times 2n}$ encodes the projection onto the unstable eigenspace, i.e. $\Psi(u - \hat{u}) = 0$ for $u \in E_s(\hat{u})$, and where T is the chosen truncation time. The calculation of Ψ at startup, which for large n turns out to be one of the bottlenecks of the algorithm, also gives a lower bound for the time scale T via $T \geq \frac{1}{-\Re\mu_1}$, where μ_1 is the eigenvalue with largest negative real part, i.e., gives the slowest direction of the stable eigenspace of $\hat{u}$. In our simulations we typically use T between 50 and 100.

In general, a BVP solver needs a good initial guess of $t \mapsto u(t)$ to solve problem (3.5). Therefore we embed problem (3.5) into a family of problems replacing (3.5b) by

$$P(0) = \alpha P_0 + (1-\alpha)\hat{P}, \quad \alpha \in [0,1], \tag{3.5d}$$

where we assume that for some α the solution is known: this holds for instance for $\alpha = 0$ with the trivial solution $u \equiv \hat{u}$. We may then gradually increase α, using the last solution as the new initial guess. This is implemented in the algorithm summarized in Table 1.

There are more sophisticated variants of the simple continuation in Step 2 of Table 1 (some of which are implemented in tt OCMat), but the simple version in general works well for the problems we considered. Nevertheless, it may be that no solution of (3.5a), (3.5c) and (3.5d) is found for $\alpha > \alpha_0$ for some $\alpha_0 < 1$, i.e., that the continuation to the intended initial point fails. In that case usually the BVP problem undergoes a fold bifurcation. We then use an adapted continuation step $2'$ that allows us to continue solutions around the fold.

Step 0	(selection of $\hat{u}$ and implementation of (3.5c)). Given $\hat{u}$ we solve the generalized adjoint eigenvalue problem $\partial_u G(\hat{u})^T \Phi = \Lambda M \Phi$ for the eigenvalues Λ and (adjoint) eigenvectors Φ, which also gives the defect $d(\hat{u})$. If $d(\hat{u}) = 0$, then from $\Phi \in \mathbb{C}^{2n\times 2n}$ we generate a real base of $E_u(\hat{u})$ which we sort into the matrix $\Psi \in \mathbb{R}^{n\times 2n}$.
Step 1	(selection of initial mesh and initial guess). To start the BVP solver we choose the initial guess $u(t) \equiv \hat{u}$ on a suitable initial grid $0 = t_0 < t_1 < \ldots < t_m = T$. Typically, we choose $m = 20$ at startup, and afterwards TOM uses its own mesh-adaption strategy.
Step 2	(solution and continuation). Using (3.5d) we try to increase α in small steps δ to $\alpha = 1$, in each step using the previous solution as the new initial guess, often trying $\delta = 1/4$. After thus having computed the first two solutions we may use a secant predictor for the subsequent steps.
Step 2'	(arclength continuation). If the continuation fails for $\alpha > \alpha_0$ with $\alpha_0 < 1$, then we use a pseudo–arclength continuation for a modified BVP, letting α be a free parameter.

Table 1: The continuation–algorithm `iscont` (Initial State Continuation); Steps 0,1 are preparatory, Step 2 or $2'$ is repeated. See [38] for implementation details, and for remarks on performance.

Remark 3.2. (a) For some applications it is useful to rescale the time $t = T\tau$ and hence consider $M\dot{u}(\tau) = TG(u(\tau)))$ on the normalized time interval $\tau \in [0, 1]$, which turns the truncation time T into a free parameter. This is for instance implemented in `OCMat`, but for simplicity not used here.

(b) Similarly to the normalized normalized objective value J_{ca} in (2.9b), in the bifurcation diagrams we use the normalized L^2 norm for comparison between different domains and space dimensions, i.e., henceforth, $\|P\|_2 := \|P\|_{L^2}/\sqrt{|\Omega|}$, and in the table in Figure 1 we present averaged values, i.e.,

$$\langle P\rangle := \frac{1}{|\Omega|}\int_\Omega P(x)\,\mathrm{d}x, \quad \langle k\rangle := \frac{1}{|\Omega|}\int_\Omega k(x)\,\mathrm{d}x. \tag{3.6}$$

To take the finite truncation time T into account we let

$$\tilde{J}(k(\cdot),T) := J(P_0(\cdot),k(\cdot,\cdot)) + \frac{\mathrm{e}^{-rT}}{r} J_{ca}(P(T),k(T)). \tag{3.7}$$

Obviously, for $T \gg \frac{1}{r}$ the last term can be made arbitrarily small, while for canonical steady state it yields the exact (discounted) objective value. In the following we drop the tilde in (3.7), and write, e.g., $J_{\hat{u}}$ for the objective value of a canonical steady state $\hat{u}$, and, e.g., $J_{P_0\to\hat{u}}$ for the canonical path which connects P_0 to $\hat{u}$.

3.2. **1D canonical steady states.** Recall that first we use tt pde2path to study the steady state problem for (3.2a), i.e.,

$$0 = -\frac{1}{q(x)} - bP(x) + \frac{P(x)^2}{1+P(x)^2} + D\Delta P(x), \tag{3.8a}$$

$$0 = 2cP(x) + q(x)\Big(r + b - \frac{2P(x)}{(1+P(x)^2)^2}\Big) - D\Delta q(x), \tag{3.8b}$$

$$\partial_\nu P(x)\big|_{\partial\Omega} = 0, \quad \partial_\nu q(x)\big|_{\partial\Omega} = 0. \tag{3.8c}$$

where additionally to (2.2) we choose the diffusion constant $D = 0.5$ as in [9], and $\Omega = (-L, L)$ in 1D. The steady states of the canonical system for the 0D model (2.1a) are FCSS of (3.8), and for easy reference we introduce the acronyms in Table 2. The FCSS are of course independent of the domain, but to search for PCSS bifurcating from FCSS, the domain size $2L$ should be close to a multiple of $2\pi/k_c$, where k_c is the wave number of a Turing like bifurcation. The parameters in (2.2), with b near 0.7, yield $k_c \approx 0.44$ [9], and for simplicity we then choose $L = 2\pi/0.44 \approx 14.28$.

name	description
FSM	Flat State Muddy, the upper FCSS branch with a high phosphor load P
FSI	Flat State Intermediate, the upper half of the second FCSS branch, intermediate P
FSC	Flat State Clean, the lower half of the second FCSS branch, low P

Table 2: Classification of the FCSS branches, see also Figure 1. The high P state is also called eutrophic, and our "muddy" refers to the fact that under eutrophic conditions there are a lot of algae and other organic matter in the lake, while the low P regime is called oligotrophic conditions, and typically gives much "cleaner" water.

Continuing the FSI branch in b we find a number of Turing like bifurcations to PCSS, and follow four of these; see Figure 1a,b for the bifurcation diagram (s), and (c) for example solutions. The notation, e.g., `p1/pt16` follows the `pde2path` scheme, e.g.: continuation step 16 on the branch p1 is stored in folder `p1` and file `pt16.mat`.

On the branches p1, p2, and p3 there are secondary bifurcations, not further considered here. For the subsequent examples we focus on $b = 0.75$ and $b = 0.65$, compute the defects $d(\hat{u})$ for all canonical steady state, and find $d(\hat{u}) = 0$ only for the FSM, for the FSC, and for some points on the p1 branch, e.g. at point 71 between the folds (see Figure 1).

(a) bifurcation diagram, (normalized) L^2 norm over b

(b) current values $J_{c,a}$ over b

(c) sample canonical steady state s

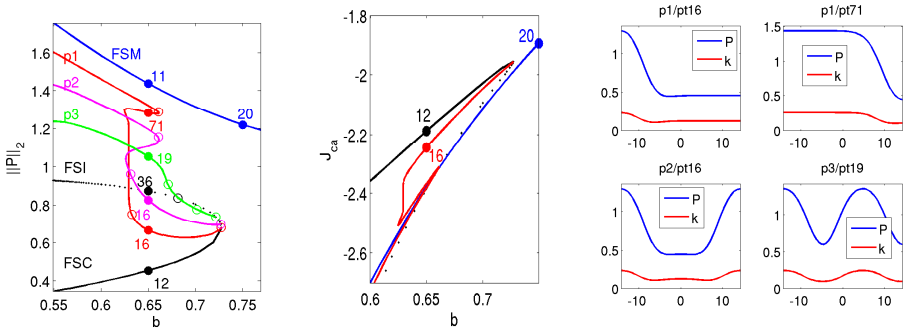

(d) Characteristics of points in (a)-(c).

name	$\langle P\rangle$	$\langle k\rangle$	J	d	name	$\langle P\rangle$	$\langle k\rangle$	J	d
FSM/pt20	1.22	0.32	-63.11	0	p1/pt16	0.61	0.14	-74.83	1
FSM/pt11	1.44	0.26	-79.28	0	p1/pt71	1.24	0.22	-78.93	0
FSI/pt36	0.87	0.13	-79.47	5	p2/pt16	0.76	0.15	-76.70	2
FSC/pt12	0.45	0.12	-72.95	0	p3/pt19	1.02	0.17	-79.48	3

Figure 1: Basic bifurcation diagrams (a) and (b), example plots (c), and characteristic values of selected canonical steady state (d). In (a), the blue and black lines represent the FCSS, and for instance the red line `p1` contains patterned canonical steady state with one "interface" between high and low P. The numbered points on all these lines correspond to selected solutions plotted in (c), and characterized in (d). The small circles in (a) denote bifurcation points. The values J_{ca} and $J = J_{ca}/r$ of the canonical steady state are all negative, but this is merely a question of offset.

3.3. **1D canonical paths.** For $b = 0.75$, the only canonical steady state is the FSM (`FSM/pt20`). It has $d(\hat{u}) = 0$, we can reach it from an arbitrary initial state P_0, and thus it is a globally stable flat optimal steady state. Therefore, this regime is not very interesting, and we immediately turn to the case $b = 0.65$ with multiple canonical steady state.

For $b = 0.65$ seven canonical steady state s are marked in Figure 1a, and characterized in the table, where only three are saddle points. These are the FSC (which has the maximal value among these canonical steady state s), the FSM, and the PCSS `p1/pt71`, subsequently denoted as $\hat{u}_{\mathrm{PS}}$. Next we numerically analyze which of these canonical steady state s belong to optimal paths.

3.3.1. *PCSS with $d(\hat{u}) > 0$.* From the analysis of non-distributed optimal control problems we know that canonical steady state s with $d(\hat{u}) > 0$ can nevertheless be optimal. To illustrate that this is at least not typical in the SLOC model, we first compare the objective value of some (arbitrary chosen) canonical steady state s, e.g., the PCSS $\hat{u}_{\mathrm{PS}^-}(\cdot)$ `p3/pt19` with $d(\hat{u}) = 3$, with that of the t–dependent canonical paths $u_i(\cdot,\cdot)$ which connect to $\hat{u}_i(\cdot)$, $i \in \{\mathrm{FSC}, \mathrm{FSM}, \mathrm{PS}\}$. For the objective values

we write J_{PS^-} for the canonical steady state, and, e.g., $J_{\mathrm{PS}^-\to\mathrm{FSC}}$ for the canonical path which goes from P_{PS^-} to $\hat{u}_{\mathrm{FSC}}$. The optimal solution for $P_0 = \hat{P}^-_{\mathrm{PS}}$ has to satisfy

$$V(\hat{P}^-_{\mathrm{PS}}) = \max\{J_{\mathrm{PS}^-},\ J_{\hat{P}^-_{\mathrm{PS}}\to\mathrm{FSC}},\ J_{\hat{P}^-_{\mathrm{PS}}\to\mathrm{FSM}},\ J_{\hat{P}^-_{\mathrm{PS}}\to\mathrm{PS}}\}. \tag{3.9}$$

The canonical paths are given in Figure 2a–c, while (d) presents some norms along the path in (a), which show that and how fast $u(t)$ (including the co–states q) converges to $\hat{u}$. In all cases we find without problems canonical paths to both FCSS and to the PCSS ; in particular the path to the FSM is rather quick.

For the objective values we find, up to 2 significant digits,

$$\begin{aligned} J_{\mathrm{PS}^-} &= -79.48 < J_{\mathrm{PS}^-\to\mathrm{FSC}} = -78.24 \\ &< J_{\mathrm{PS}^-\to\mathrm{PS}} = -78.19 < J_{\mathrm{PS}^-\to\mathrm{FSM}} = -77.5. \end{aligned} \tag{3.10}$$

Thus, the optimal path is the one converging to $\hat{u}_{\mathrm{FSM}}$. Repeating these steps for every PCSS with $d(\hat{u}) > 0$ we find that these are always dominated by paths converging to one of the FCSS. Therefore, only $\hat{u}_{\mathrm{FSC}}$, $\hat{u}_{\mathrm{FSM}}$ and $\hat{u}_{\mathrm{PS}}$ remain as candidates for optimal steady state.

Before we turn to determining optimal steady states we briefly discuss the canonical paths in Figure 2. We focus on (a), but similar remarks apply to (b,c) as well. In (a), the initial $P(\cdot, 0)$ is above the target $\hat{P}_{\mathrm{FSC}}$, so naively we may expect that the control k should start below the target $\hat{k}_{\mathrm{FSC}}$ and slowly increase to $\hat{k}_{\mathrm{FSC}}$. However, such a control would not be optimal. Instead, k is initially similar to $\hat{k}_{\mathrm{PS}^-}$, and in particular $k(\cdot, 0)$ is large where $P_0(\cdot)$ is already large. Only after a short transient k drops below $\hat{k}_{\mathrm{FSC}}$ and then behaves as expected.

At first sight, this startup behavior of k may appear rather counter–intuitive. However, the reason is that we do *not* want to drive the system to $\hat{u}_{\mathrm{FSC}}$ "as quickly as possible", which essentially would amount to choosing k "as small as possible" at startup. Instead, we want to maximize J, and for this it pays off to have, for a short transient, k large near the maxima of $P(\cdot, 0)$. To illustrate this point, in Figure 2(e) we *choose* the naive control $k(t) \equiv k_{\mathrm{FSC}}$ for all t and numerically integrate the *initial value problem* (2.9c). While this does take us to $\hat{u}_{\mathrm{FSC}}$, the first observation is that this needs a rather long time. Secondly, for the value of this solution we obtain $J = -80.1$, which is even worse than the starting canonical steady state with $J_{\mathrm{PS}^-} = -79.48$.

3.3.2. *Determining optimal steady states.* We return to the question whether one or more of the saddle point canonical steady state s at $b = 0.65$ are optimal, and proceed in three steps. First we search for a canonical path starting at $\hat{P}_{\mathrm{PS}}$ and connecting to $\hat{u}_{\mathrm{FSC}}$. In the second step we repeat that for $\hat{u}_{\mathrm{FSM}}$, and in the last step we check if both or only one of the FCSS are optimal. The second step reveals that the first step is superfluous, but this we do not know a priori.

Paths between $\hat{P}_{\mathrm{PS}}$ and $\hat{u}_{\mathbf{FSC}}$ – a Skiba candidate. Using `iscont` to get a canonical path starting at $\hat{P}_{\mathrm{PS}}$ and converging to the FSC it turns out that the continuation (3.5d), i.e.,

$$P_\alpha(0) := \alpha P_{\mathrm{PS}} + (1-\alpha) P_{\mathrm{FSC}}, \tag{3.11}$$

yields a fold around $\alpha \approx 0.6$, see the blue curve in Figure 3a), and that no canonical path connecting $\hat{P}_{\mathrm{PS}}$ to $\hat{u}_{\mathrm{FSC}}$ exists. Instead, multiple solutions that converge to

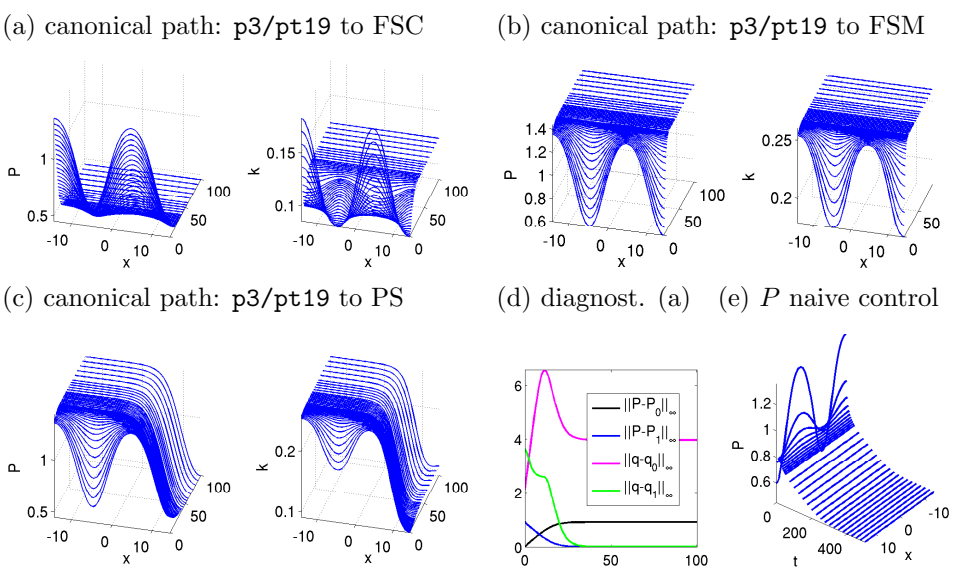

Figure 2: Canonical paths from the (state values of) PCSS nspp p3/pt19 to FSC (a), FSM (b), and PS (c) at $b = 0.65$, and typical path diagnostics (d). For comparison, (e) shows the solution P of the initial value problem (2.9c) with $P(0)$ as in (a) and the externally chosen control $k(t) \equiv k_{\mathrm{FSC}}$ for all t.

$\hat{u}_{\mathrm{FSC}}$ exist for initial distributions of the form (3.5d) with $\alpha \in [0.6, 0.71]$; two examples are shown in Figure 3b, and their diagnostics in (c).

Similarly, trying to continue to a path that connects $\hat{P}_{\mathrm{FSC}}$ and $\hat{u}_{\mathrm{PS}}$ yields a fold (green curve in (a)), and no such path exists. However, the solutions returned during the continuation process allow us to determine and compare the respective objective values. This yields that there exists a specific initial distribution P_S where the objective values are equal, given by the intersection of the green and blue curves in Figure 3a. Thus, from an economic point of view both solutions are equal. This suggests that P_S is a Skiba or indifference threshold point (distribution), well known from non-distributed optimal control problems, see, e.g., [42, 21]. However, taking into account also the FSM solution, below we identify P_S as only a Skiba candidate.

The paths u starting at P_S (red curve) are depicted in Figure 3d: $P(\cdot, 0)$ is the same for both solutions, but the controls $k(\cdot, 0)$ are different. In any case, to assure that these solutions are optimal we have to prove that no other dominating solution exists. Thus in a last step we calculate the objective values of the paths converging to $\hat{u}_{\mathrm{FSM}}$.

From $\hat{P}_{\mathrm{PS}}$ to $\hat{u}_{\mathrm{FSM}}$. Here the continuation is successful and we find a path connecting $\hat{P}_{\mathrm{PS}}$ to $\hat{u}_{\mathrm{FSM}}$. Comparing the objective values reveals that $\hat{u}_{\mathrm{PS}}$ is dominated by this path, see Figure 3e and 3f. Thus, the $\hat{u}_{\mathrm{PS}}$ is ruled out as an optimal steady state, and therefore we a posteriori identify P_S as only a Skiba *candidate* as it does *not* separate two optimal steady states.

A Skiba manifold between $\hat{P}_{\mathrm{FSM}}$ and $\hat{P}_{\mathrm{FSC}}$. It is well known that in 0D the FSC and FSM are only locally stable with regions of attractions separated by a Skiba

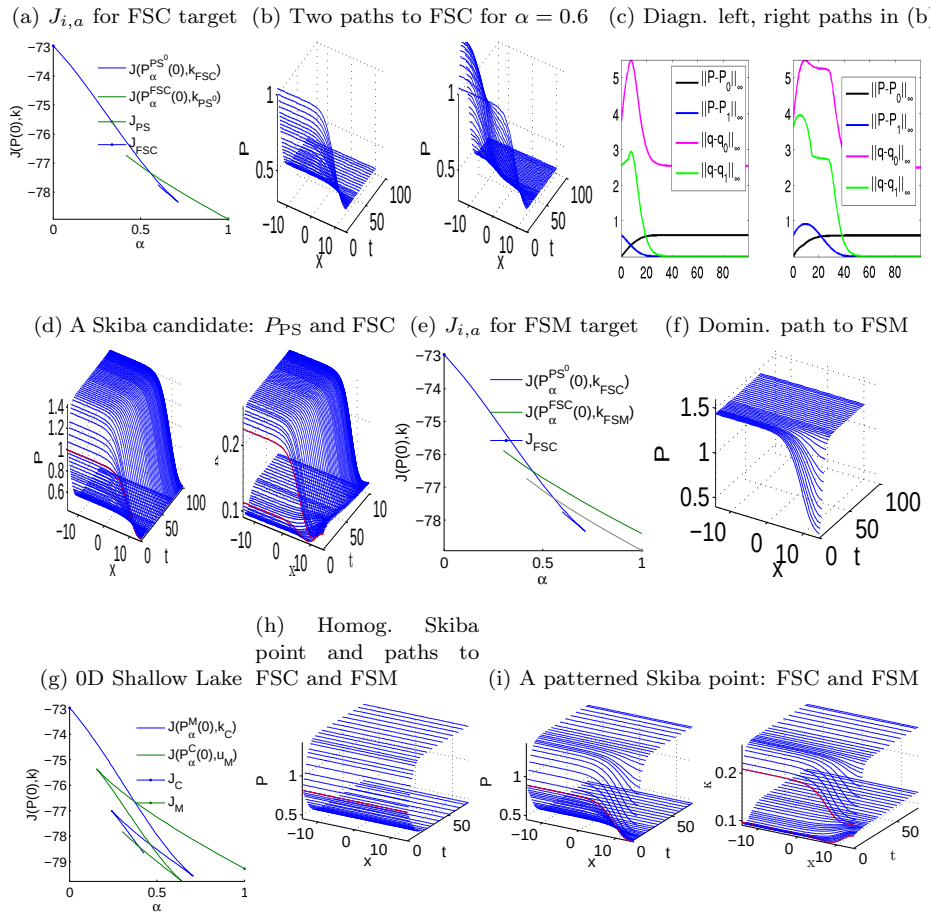

Figure 3: Canonical paths to various canonical steady state for $b = 0.65$, and illustration of some Skiba points; see text for details.

manifold (parametrized by, e.g., b) of homogeneous solutions, [21], see Figure 3g for our case $b = 0.65$. Of course, this also yields a homogeneous Skiba distribution in 1D, see Figure 3h. More generally, we may expect the domains of attraction of the FSC and the FSM to be separated by a Skiba manifold M_S, which in the continuum limit becomes infinite dimensional.

A continuation process, analogous to the non-distributed case, see [17], could be used to approximate this manifold M_S. However, to find a non homogeneous example point on that manifold, here we can readily combine Figure 3a and 3e, to find a Skiba distribution of the form

$$P_{\rm Skiba} = \alpha \hat{P}_{\rm FSC} + (1-\alpha)\hat{P}_{\rm PS}; \tag{3.12}$$

see Figure 3i for paths to the FSC and the FSM yielding the same $J = -76.3$.

Summary for 1D. The picture that emerges is as follows: for $b > b_{\rm fold} \approx 0.727$ the FSM as the only canonical steady state is the globally stable optimal steady

state, while for $b < b_{\rm fold}$ there exist multiple canonical steady state. Specifically for $b = 0.65$, $\hat{u}_{\rm FSC}, \hat{u}_{\rm FSM}$ and one of the PCSS are saddle points, but only $\hat{u}_{\rm FSC}$ and $\hat{u}_{\rm FSM}$ are optimal, and in particular no patterned optimal steady state s exist. The flat optimal steady state s FSC and FSM are separated by a (presumably rather complicated) Skiba manifold M_S, and Figure 3h and 3i show just two examples of points on M_S.

3.4. **Outlook: 2D results.** As a 2D example we consider (2.11) on the domain $\Omega = (-L, L) \times (-L/2, L/2)$, $L = 2\pi/0.44$ as before, with a rather coarse mesh of 40×20 points, hence approximately 1600 DoF. The FCSS branches are of course the same as in 1D (or 0D), and again at the end of the FSI branch we find a number of Turing like bifurcations. In Figure 4(a),(b) we only present the "new" patterned branches, i.e., those with a genuine x and y dependence.

(a) Two 2D PCSS branches

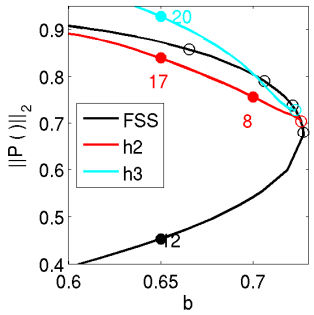

(b) some example plots

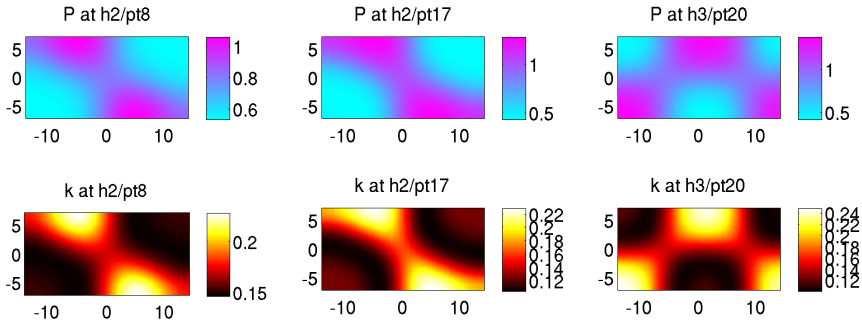

Figure 4: New patterned branches in 2D; $(x, y) \in (-L, L) \times (-\frac{L}{2}, \frac{L}{2})$.

These new bifurcating PCSS have $d(\hat{u}) > 0$. As an example for a canonical path, in Figure 5 we present snapshots from a path from $\hat{P}$ of the PCSS `h2/pt17` to the FSC, which yields a higher J than the PCSS , i.e.,

$$J(\text{PCSS}) = -77.53 < J(\text{PCSS} \to \text{FSC}) = -76.23 < J(\text{FSC}) = -72.97. \quad (3.13)$$

Thus, this PCSS is not optimal, and neither is any other one we checked. Using the methods from §3.2 it is now of course also possible to find points with a genuine

x and y dependence on the Skiba manifold separating FSC and FSM, but here we skip this presentation.

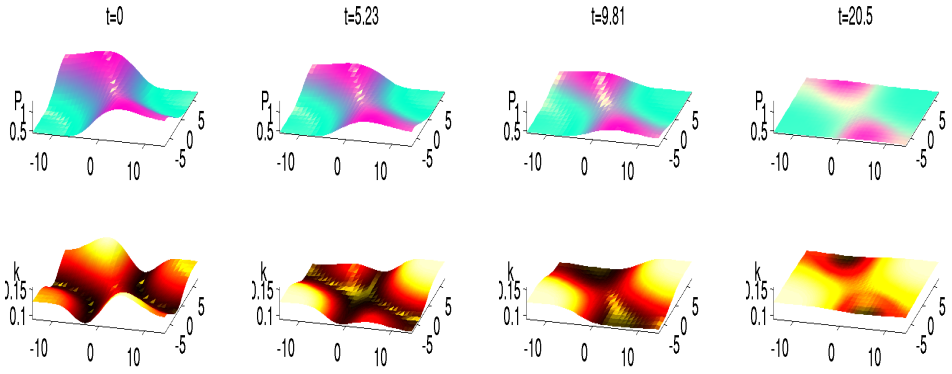

Figure 5: Solutions on the canonical path to FSC

The behavior and economic interpretation of the path from the PCSS to FSC in Figure 5 is rather similar to the convergence to FSC in Figure 2a. After a short transient the optimal strategy is to give a high phosphate load k where P is below the limit value $\hat{P}_{\mathrm{FSC}}$ (south-west and north-east corners of the domain), but initially there also is a high k at high P values (north-west and south-east corners).

4. Discussion

We have presented a numerical framework to treat infinite time horizon spatially distributed optimal control problems. First we derive the canonical PDE systems, which we then discretize in space and thus approximate by large systems of ODEs. For these we can resort to the theory and experience with non-distributed optimal control problems. Thus our results are intrinsically numerical; however, we believe that they can help to develop the theoretical concepts for distributed optimal control problems.

From the economic point of view, the computation of canonical paths to the flat optimal steady state s yields nontrivial and interesting results. Even more interesting would be locally stable patterned optimal steady state s, but there is strong evidence that these do not exist for the shallow lake model (2.9), at least in the parameter regimes we considered so far. See however "Scenario 2" in [18] for some locally stable patterned optimal steady state s.

On the other hand, in [39] we use our method to study the vegetation system from [7], and find that patterned optimal steady state s dominate in large parameter regimes. We believe that the same happens in many other important systems. Natural candidates, i.e., systems with natural objective functions and controls, are related vegetation systems as in [34, 43], fishery models as in [29, 17], or "crimotaxis" systems as in [35].

5. Appendix: Saddle point property for PDEs

In this appendix we discuss the saddle point property (Definition 3.1) in a somewhat more general situation, tailored to canonical systems coming from spatial discretizations of PDEs. Let $\hat{u} = (\hat{p}, \hat{q}) \in \mathbb{R}^{2N}$ be a stationary state of a (non–distributed) canonical system of the form

$$\frac{\mathrm{d}}{\mathrm{d}t}\begin{pmatrix} p \\ q \end{pmatrix} = F(p,q) := \begin{pmatrix} f(p,q) \\ rq - H_p(p,q)) \end{pmatrix}, \tag{5.1}$$

where $f = H_q$, and let $J = D_u F(\hat{u})$ be the Jacobian at $\hat{u}$. In [19, Thm 7.10] it is explained that the eigenvalues of J are symmetric around $r/2$, i.e., that there exist N complex numbers ξ_i such that

$$\sigma(J) = \big\{ \frac{r}{2} \pm \xi_i : i = 1, \dots, N \big\}. \tag{5.2}$$

In detail, since $\det(J - \xi) = \det(J_r - (\xi - \frac{r}{2}))$ where

$$J_r := J - \frac{r}{2} = \begin{pmatrix} H_{pq} - \frac{r}{2} & H_{qq} \\ -H_{pp} & -H_{pq} + \frac{r}{2} \end{pmatrix}, \tag{5.3}$$

we have that $\frac{r}{2} + \xi_i \in \mathbb{C}$ is an eigenvalue of J if and only if ξ_i is an eigenvalue of J_r. But J_r has the structure $\begin{pmatrix} A & B \\ \mathbb{C} & -A \end{pmatrix}$ with symmetric matrices $B, C \in \mathbb{R}^{N\times N}$, and as a consequence the eigenvalues of J_r are $\xi_i = \pm\sqrt{\tilde{\xi}_i}$, $i = 1, \dots, N$.

Now we consider the distributed canonical system

$$\partial_t \begin{pmatrix} p(x,t) \\ q(x,t) \end{pmatrix} = F(p(x,t), q(x,t)) + \begin{pmatrix} D\Delta p(x,t) \\ -D\Delta q(x,t) \end{pmatrix}, \tag{5.4}$$

where $D \in \mathbb{R}^{N\times N}$ is a diffusion matrix, i.e., positive definite. Let

$$\frac{\mathrm{d}}{\mathrm{d}t} u(t) = G(u(t)), \quad u \in \mathbb{R}^{2nN}, \tag{5.5}$$

be the associated spatially discretized system with n spatial points, where $u = (p(x_1), \dots, p(x_n), q(x_1), \dots, q(x_n)) \in \mathbb{R}^{2nN}$, and let $\hat{u} \in \mathbb{R}^{2nN}$ be a steady state of (5.5). Then $J = D_u G(\hat{u})$ has the structure $J = -K + J_{\mathrm{local}}$, where J_{local} has the block structure

$$J_{\mathrm{local}} = \begin{pmatrix} H^1_{pq} & 0 & \dots & 0 & H^1_{qq} & 0 & \dots & 0 \\ 0 & H^2_{pq} & \dots & 0 & 0 & H^2_{qq} & \dots & 0 \\ \vdots & \vdots & \ddots & \dots & \vdots & \vdots & \ddots & \vdots \\ 0 & 0 & \dots & H^n_{qq} & 0 & 0 & \dots & H^n_{qq} \\ -H^1_{pp} & 0 & \dots & 0 & r - H^1_{qp} & 0 & \dots & 0 \\ 0 & -H^2_{pp} & \dots & 0 & 0 & r - H^2_{qp} & \dots & 0 \\ \vdots & \vdots & \ddots & \dots & \vdots & \vdots & \ddots & \vdots \\ 0 & 0 & \dots & -H^n_{pp} & 0 & 0 & \dots & r - H^n_{qp} \end{pmatrix},$$

composed of local matrices $H^j_{pq} := H_{pq}(p(x_j), q(x_j)), H^j_{qq}, H^j_{pp} \in \mathbb{R}^{N\times N}$, and $K = \begin{pmatrix} L & 0 \\ 0 & -L \end{pmatrix}$ with $L \in \mathbb{R}^{nN}$ coming from the discretization of $D\Delta$. The notation K of course reflects the finite element background of the present paper, but the same

structure $\begin{pmatrix} L & 0 \\ 0 & -L \end{pmatrix}$ occurs for any discretization, in any space dimension, and for any D not necessarily diagonal, i.e., containing cross diffusion.

It follows that again $\frac{r}{2} + \xi_i$ is an eigenvalue of J if and only if ξ is an eigenvalue of $J_r := J - \frac{r}{2}$, where J_r has the structure

$$J_r = \begin{pmatrix} A & B \\ C & -A \end{pmatrix},$$

with symmetric matrices $B, C \in \mathbb{R}^{nN}$. Applying [19, Lemma B.2, Lemma B.3] we obtain the following result.

Theorem 5.1. *Let $\hat{u}$ be a steady state of the spatially discretized distributed system (5.5), and let J be the associated Jacobian. Then there exist $\xi_i \in \mathbb{C}$, $i = 1, \dots, nN$, such that*

$$\sigma(J) = \big\{ \frac{r}{2} \pm \xi_i : i = 1, \dots, nN \big\}. \tag{5.6}$$

As a consequence, $\dim E_s(\hat{u}) \leq Nn$, and the only candidates $\hat{u}$ for right BC in (3.5c) are those with $d(\hat{u}) = 0$. As a corollary we find a property that, on the discretized level, is equivalent to $d(\hat{u}) = 0$.

Corollary 5.2. *Let $\hat{u} \in \mathbb{R}^{2nN}$ be an equilibrium of the spatially discretized distributed system (5.5) and $r > 0$. Then $d(\hat{u}) = 0$ if and only if every eigenvalue ξ of the Jacobian $J(\hat{u})$ satisfies*

$$\|\Re\xi - \frac{r}{2}\| > \frac{r}{2}. \tag{5.7}$$

Theorem 5.1 is formulated on the discretized level, and the question is how it ultimately relates to the PDE. As a first step one can ask: Let a steady state $\hat{u} \in \mathbb{R}^{2nN}$ of (5.5) be an approximation of a PDE steady state $(\hat{p}, \hat{q}) \in X$ for (5.4), with $X \subset \{(p, q) : \Omega \to \mathbb{R}^{2N}\}$ some function space, e.g., $X = [H^1(\Omega)]^{2N}$. If $\tilde{\hat{u}} \in \mathbb{R}^{2\tilde{n}N}$ is an approximation of $(\hat{p}, \hat{q})$ on a finer mesh $\tilde{n} > n$, or just a different mesh, do we have

$$nN - \dim E_s(\hat{u}) = \tilde{n}N - \dim E_s(\tilde{\hat{u}}) \quad ? \tag{5.8}$$

Heuristically, if $E_c(\hat{u}) = \emptyset$, i.e., $\sigma(J) \cap \{\mathrm{Re}\xi = 0\} = \emptyset$, then (5.8) is true, for large enough $n, \tilde{n}$. Given some $\hat{u}$, this can be easily tested numerically, and it is also clear from an analytical point of view. Refining $\hat{u}$ to $\tilde{\hat{u}}$ we essentially add high frequency modes to the mesh. These introduce the same number of additional eigenvalues at large positive and negative ξ for the linearization $\tilde{J}$, because $J_F(p, q) : X \to X$ is relatively compact with respect to the Laplacian, i.e., w.r.t. $(p, q) \mapsto (D\Delta p, -D\Delta q)$. On the other hand, the small eigenvalues μ_i, $|\mu_i| < R$ for some fixed R, are only slightly perturbed, i.e., $|\mu_i - \tilde{\mu}_i| \leq C\|\hat{u}_* - \tilde{\hat{u}}\|$, where $\hat{u}_*$ is suitably defined, for instance by interpolating $\hat{u}$ to the mesh of $\tilde{\hat{u}}$. But $\|\hat{u}_* - \tilde{\hat{u}}\| \to 0$ as $n, \tilde{n} \to \infty$, which yields a positive answer to (5.8).

To make this rigorous, we need to define appropriate function spaces and study the approximation properties of the spatial discretization. This is easy, as the stationary problem for (5.4) can be written as an elliptic system, and hence (p, q) is arbitrary smooth, but we omit the details here.

Importantly, (5.7) can also be formulated on the PDE level and might therefore replace the saddle point property from Definition 3.1 for spatially distributed models. However, we also postpone an in depth analysis of this to future work.

References

[1] S. Aniţa, V. Arnăutu, V. Capasso; *An introduction to optimal control problems in life sciences and economics*, Birkhäuser/Springer, New York, 2011.

[2] S. Aniţa, V. Capasso, H. Kunze, D. La Torre; *Optimal control and long-run dynamics for a spatial economic growth model with physical capital accumulation and pollution diffusion*, Appl. Math. Lett., **26** (2013), no. 8, 908–912.

[3] N. Apreutesei, G. Dimitriu, R. Strugariu; *An optimal control problem for a two-prey and one-predator model with diffusion*, Comput. Math. Appl., **67** (2014), no. 12, 2127–2143.

[4] S. Aseev and A. Kryazhimskii; *The Pontryagin maximum principle and optimal economic growth problems*, Proceedings of the Steklov Institute of Mathematics, **257** (2007), no. 1, 1–255.

[5] S. Aseev and V. Veliov; *Maximum principle for infinite-horizon optimal control problems with dominating discount*, Dyn. Contin. Discrete Impuls. Syst. Ser. B Appl. Algorithms, **19** (2012), no. 1-2, 43–63.

[6] W.J. Beyn, Th. Pampel, W. Semmler; *Dynamic optimization and Skiba sets in economic examples*, Optimal Control Applications and Methods, **22** (2001), no. 5–6, 251–280.

[7] W. Brock and A. Xepapadeas; *Pattern formation, spatial externalities and regulation in coupled economic–ecological systems*, Journal of Environmental Economics and Management, **59** (2010), no. 2, 149–164.

[8] W.A. Brock and A. Xepapadeas; *Diffusion-induced instability and pattern formation in infinite horizon recursive optimal control*, 2006, Preprint, available at SSRN: http://ssrn.com/abstract=895682.

[9] W.A. Brock, A. Xepapadeas; *Diffusion-induced instability and pattern formation in infinite horizon recursive optimal control*, Journal of Economic Dynamics and Control, **32** (2008), no. 9, 2745–2787.

[10] D. A. Carlson, A. Haurie; *Infinite horizon optimal control*, Lecture Notes in Economics and Mathematical Systems, vol. 290, Springer-Verlag, Berlin, 1987, Theory and applications.

[11] S.R. Carpenter, W. A. Brock; *Spatial complexity, resilience and policy diversity: fishing on lake-rich landscapes*, Ecology and Society, **9** (2004), no. 1.

[12] C. W. Clark; *Mathematical bioeconomics*, second ed., John Wiley & Sons, Inc., New York, 1990, The optimal management of renewable resources.

[13] W. Ding, V. Hrynkiv, X. Mu; *Optimal control applied to native–invasive species competition via a PDE model*, Electron. J. Differential Equ., **2012** (2012), no. 237, 1–18.

[14] W. Ding and S. Lenhart; *Optimal harvesting of a spatially explicit fishery model*, Natural Resource Modeling, **22** (2009), no. 2, 173–211.

[15] E. Doedel, A. R. Champneys, Th. F. Fairgrieve, Y. A. Kuznetsov, Bj. Sandstede, X. Wang; *AUTO: Continuation and bifurcation software for ordinary differential equations (with HomCont)*, http://cmvl.cs.concordia.ca/auto/, 1997.

[16] T. Dohnal, J. Rademacher, H. Uecker, D. Wetzel; *pde2path 2.0*, ENOC 2014 - Proceedings of 8th European Nonlinear Dynamics Conference, ISBN: 978-3-200-03433-4 (H. Ecker, A. Steindl, and S. Jakubek, eds.), 2014.

[17] D. Grass; *Numerical computation of the optimal vector field in a fishery model*, Journal of Economic Dynamics and Control, **36** (2012), no. 10, 1626–1658.

[18] D. Grass; *From 0D to 1D spatial models using OCMat*, Tech. report, ORCOS, 2015.

[19] D. Grass, J.P. Caulkins, G. Feichtinger, G. Tragler, D.A. Behrens; *Optimal control of nonlinear processes: With applications in drugs, corruption, and terror*, Springer Verlag, 2008.

[20] T. Kiseleva; *Structural analysis of complex ecological economic optimal control problems*, Ph.D. thesis, University of Amsterdam, Center for Nonlinear Dynamics in Economics and Finance (CeNDEF), 2011.

[21] T. Kiseleva, F. O. O. Wagener; *Bifurcations of optimal vector fields in the shallow lake system*, Journal of Economic Dynamics and Control, **34** (2010), no. 5, 825–843.

[22] S. Lenhart, J. Workman; *Optimal control applied to biological models*, Chapman Hall, 2007.

[23] M. Lentini, H. B. Keller; *Boundary value problems on semi-infinite intervals and their numerical solution*, SIAM Journal on Numerical Analysis, **17** (1980), no. 4, 577–604.

[24] X. Li, J. Yong; *Optimal control theory for infinite dimensional systems*, Birkhäuser, Boston, 1995.

[25] J. L. Lions; *Optimal control of systems governed by partial differential equations*, Springer-Verlag, New York, 1971.
[26] K. G. Mäler, A. Xepapadeas, A. de Zeeuw; *The economics of shallow lakes*, Environmental and Resource Economics, **26** (2003), no. 4, 603–624.
[27] F. Mazzia, A. Sestini, D. Trigiante; *The continuous extension of the B-spline linear multistep methods for BVPs on non-uniform meshes*, Applied Numerical Mathematics, **59** (2009), no. 3–4, 723–738.
[28] F. Mazzia, I. Sgura; *Numerical approximation of nonlinear BVPs by means of BVMs*, Applied Numerical Mathematics **42** (2002), no. 1–3, 337–352, Numerical Solution of Differential and Differential-Algebraic Equations, 4-9 September 2000, Halle, Germany.
[29] M. G. Neubert; *Marine reserves and optimal harvesting*, Ecology Letters **6** (2003), no. 9, 843–849.
[30] L. S. Pontryagin, V. G. Boltyanskii, R. V. Gamkrelidze, E. F. Mishchenko; *The mathematical theory of optimal processes*, Wiley-Interscience, New York, 1962.
[31] J. P. Raymond, H. Zidani; *Hamiltonian Pontryagin's principles for control problems governed by semilinear parabolic equations*, Appl. Math. Optim., **39** (1999), no. 2, 143–177.
[32] J. P. Raymond, H. Zidani; *Pontryagin's principle for time-optimal problems*, J. Optim. Theory Appl., **101** (1999), no. 2, 375–402.
[33] M. Scheffer; *Ecology of Shallow Lakes*, Kluwer Academic Publishers , 1998.
[34] M. Shachak, Y. Zarmi, J. von Hardenberg, E. Meron; *Diversity of vegetation patterns and desertification*, PRL **87** (2001).
[35] M. B. Short, A. L. Bertozzi, P. J. Brantingham; *Nonlinear patterns in urban crime: hotspots, bifurcations, and suppression*, SIAM J. Appl. Dyn. Syst., **9** (2010), no. 2.
[36] N. Tauchnitz; *The Pontryagin maximum principle for nonlinear optimal control problems with infinite horizon*, J. Optim. Theory Appl., **167** (2015), no. 1, 27–48.
[37] Fredi Tröltzsch; *Optimal control of partial differential equations*, Graduate Studies in Mathematics, vol. 112, American Mathematical Society, Providence, RI, 2010.
[38] H. Uecker; *The pde2path add-on library p2poc for solving infinite time-horizon spatially distributed optimal control problems — Quickstart Guide*, Preprint, 2015.
[39] H. Uecker; *Optimal harvesting and spatial patterns in a semi arid vegetation system*, Natural Resource Modelling **29** (2016), no. 2, 229–258.
[40] H. Uecker; *pde2path, www.staff.uni-oldenburg.de/hannes.uecker/pde2path*, 2016.
[41] H. Uecker, D. Wetzel, and J. Rademacher, *pde2path – a Matlab package for continuation and bifurcation in 2D elliptic systems*, NMTMA **7** (2014), 58–106.
[42] F. O. O. Wagener; *Skiba points and heteroclinic bifurcations, with applications to the shallow lake system*, Journal of Economic Dynamics and Control, **27** (2003), no. 9, 1533–1561.
[43] Y. Zelnik, S. Kinast, H. Yizhaq, G. Bel, E. Meron; *Regime shifts in models of dryland vegetation*, Philos. Trans. R. Soc. Lond. Ser. A Math. Phys. Eng. Sci., **371** (2013), no. 2004.

Dieter Grass
ORCOS, Institute of Mathematical Methods in Economics, Vienna University of Technology, A-1040 Vienna, Austria
E-mail address: dieter.grass@tuwien.ac.at

Hannes Uecker
Institut für Mathematik, Universität Oldenburg, D26111 Oldenburg, Germany
E-mail address: hannes.uecker@uni-oldenburg.de